New Early Permian paleomagnetic results from the Brive basin (French Massif Central) and their implications for Late Variscan tectonics.

Yan Chen, Bernard Henry, Michel Faure, Jean-François Becq-Giraudon, Jean-Yves Talbot, Lucien Daly, Maxime Le Goff

New Early Permian paleomagnetic results from the Brive basin (French Massif Central) and their implications for Late Variscan tectonics

Yan Chen[1] , Bernard Henry[2], Michel Faure[1], Jean-François Becq-Giraudon[3],

Jean-Yves Talbot[1], Lucien Daly[2] and Maxime Le Goff[2]

(1) Institut des Sciences de la Terre d'Orléans, Université d'Orléans, 45067 Orléans cedex 02, France

(2) Géomagnétisme et Paléomagnétisme, IPGP and CNRS, 4 avenue de Neptune, 94107 Saint Maur cedex, France

(3) BRGM-DR/MGG, 46060 Orléans cedex 02, France

Abstract

In order to assess the structural evolution of the Brive basin and the Paleozoic activity of surrounding major faults in the French Massif Central, we carried out a paleomagnetic study on Early Permian rocks from this basin. Positive-fold tests and solely reversed polarities indicate that the characteristic remanent magnetization is likely to be primary. Early Permian tilt-corrected site mean declinations vary from 207°–167° indicating that the Brive basin experienced internal vertical-axis rotations. On the contrary, Late Permian paleomagnetic site means exhibit a circular Fisherian distribution showing no relative rotations. Detailed analyses of Permian paleomagnetic data from five contemporaneous basins of the French Massif Central reveal that these basins share the same equatorial paleolatitude with stable Europe throughout the Permian. However, in Early Permian, three of the five basins experienced differential rotations. The Saint-Affrique basin not only suffered internal deformation during the Early Permian, but the basin as a whole underwent a full-scale counterclockwise vertical-axis block rotation with respect to stable Europe. As a consequence, paleomagnetic data from similar late orogenic basins have to be thus carefully considered for establishment of Apparent Polar Wander paths.

Keywords Brive basin - French Massif Central - Paleomagnetism - Permian - Stable Europe

Introduction

The Variscan orogeny is the most important Paleozoic tectonic event in Western Europe, and the French Massif Central contains among the best exposures to observe the deformation related to this event. It is now well acknowledged that nappe stacking, metamorphism and magmatism took place during the convergence between Gondwana, Laurussia and several microcontinents, and that the collision was completed in the Early Carboniferous (e.g., Matte *1986*; Autran and Cogné *1980*). The Middle to Late Carboniferous post-collisional evolution of the belt is characterized by two successive extensional stages (Faure *1995*). The first one, beginning in the Late Visean (ca. 330 Ma), is coeval with Namurian-Westphalian synkinematic plutonism. The second one, from the Late Carboniferous to the Early Permian, is associated with the opening of several coal-bearing intramontane half-graben basins deposited on the metamorphic basement (Fig. 1a). NE–SW stretching directions characterize the Late Carboniferous-Early Permian extension. Some major faults, such as the Cévennes, Sillon Houiller and Argentat faults, played an important role to accommodate the extension. The Sillon Houiller fault is a major discontinuity at the scale of the Variscan Belt of Europe. For this fault, a Late Carboniferous left-lateral displacement of about 50 km is documented on the basis of offset of geological features (plutons, faults, metamorphic series, etc., e.g., Grolier and Letourneur *1968*; Blès et al. *1989*).

However, younger movements along these major faults remain undocumented, though Late Permian extension is clear in some Permian basins (Bourges *1987*). Moreover, the reality of post-Permian activity along the Sillon Houiller appears highly likely. Indeed, since 250 Ma, the French Massif Central experienced several continental-scale tectonic such as Early Mesozoic rifting related to the formation of the passive margin of the Alpine Ligurian-Piemontese Ocean, the Eocene Pyrenean compression and the Oligocene-Miocene intracontinental rifting. In addition, paleomagnetism pointed out, for example, local small block rotations during Pyrenean tectonics in the eastern part of the Massif Central, close to the Cévennes faults (Henry et al. *2004*).

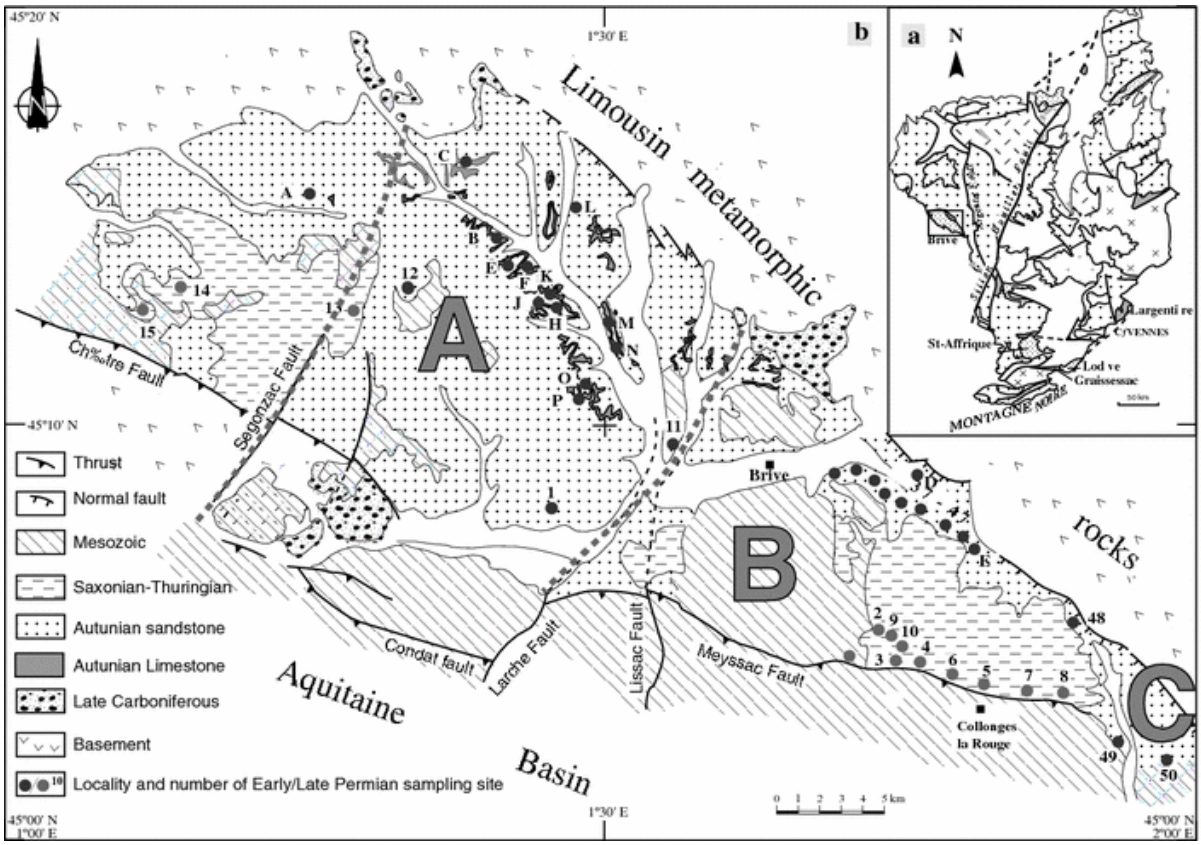

Fig. 1 A sketch of tectonic map of the French Massif Central **a** and schematic geological map of the Brive basin **b** (after Lefavrais-Raymond and Feys 1976)

Thus, its application to the Brive basin might be a key tool to bring constraints on possible displacements along Argentat and Sillon Houiller faults. The interest of such a study is also of more general order. In fact, a significant part of paleomagnetic data used to establish Apparent Polar Wander Path (APWP) for the main continents and thus the continental drifts have been obtained in detrital basins around orogenic areas. This is particularly true for Upper Paleozoic times. To point out local rotations within such basins should imply to reconsider in detail part of these paleomagnetic reference poles.

The paleomagnetic studies carried out in the Lodève (Mérabet and Guillaume *1988*; Henry *1988*) and Largentière (Henry et al. *1999*) Permian basins on the southeastern border of Massif Central revealed that they were rigidly attached to stable Europe since at least Early Permian. But paleomagnetic results from other contemporaneous Permian basins in the southwestern French Massif Central, such as the Saint-Affrique (Cogné et al. *1990*, *1993*, Diego-Orozco and Henry *1993*), and the Rodez basins (Diego-Orozco et al. *2002*) show rotations at different scales during the Permian. During the Early Permian, the Saint-Affrique

Basin experienced internal deformation characterized by paleomagnetic block rotations and a strong counterclockwise rotation is also suspected in the Rodez Basin. It was then important to determine if Saint-Affrique and Rodez basins represent exceptional cases or if similar rotations can be observed in other basins. In a previous paleomagnetic study of the Brive Basin, only three sites of 15 concern Early Permian rocks (Chen et al. *1997*). To get a better understanding of the kinematics of the Brive basin and to infer the Paleozoic or even younger activity of the surrounding faults, a paleomagnetic study of the Early Permian rocks from this basin has been then carried out.

Geological setting and paleomagnetic sampling

The Carboniferous–Permian Brive basin is situated on the southwestern border of the French Massif Central (Fig. 1a). This NW–SE elongated basin of about 600 km2 overlies the Limousin metamorphic basement and is unconformably overlain by sub-horizontal Triassic and Jurassic formations. Although locally the northeastern border is a normal fault, the primary contact is stratigraphic, because Carboniferous and Permian rocks unconformably cover the metamorphic rocks with a basal conglomerate and coarse sandstone (Fig. 2). The southern border is truncated by a series of WNW–ESE trending reverse faults (Fig. 1b). Drilling has identified Permian rocks extending farther south under the Mesozoic strata, up to the Figeac area (Fig. 1a). This agrees with sedimentological studies that show a southwestward thickening and coarsening of the deposits (Feys et al. *1979*; Feys *1989*). The Châtre, Meyssac and Condat faults belong to the same system of WNW–ESE trending Late Variscan structures offset by the NNE–SSW Segonzac and Larche strike-slip faults and by the N-S Lissac strike-slip fault (Fig. 1b). Although all these faults were reactivated as left lateral wrench faults during the Tertiary Pyrenean compression, detailed facies analyses of Permian deposits support a Late Paleozoic motion, responsible for the diversity of sedimentary in-filling. The southward deepening Carboniferous–Permian sediments indicate an asymmetric shape for the Brive basin. Such a geometry is in agreement with the half-graben structure observed in most of Late Paleozoic basins of the French Massif Central (e.g., Faure *1995*). An extensional setting appears likely for the origin of this basin.

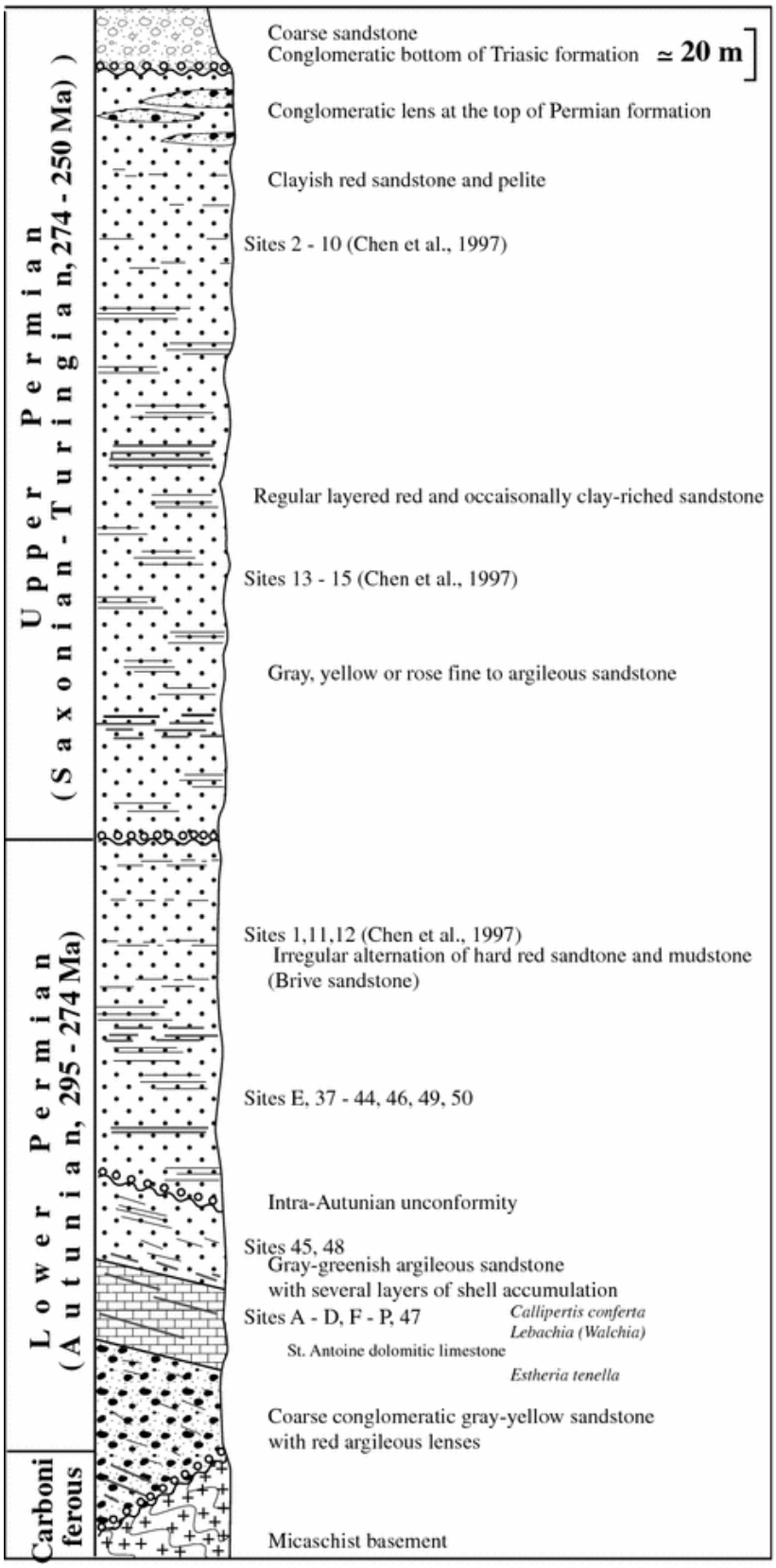

Fig. 2 Stratigraphic log of the Brive basin with fossil occurrences and sampling site locations (after BRGM *1989*)

The history of the Brive basin begins with the opening of the WNW–ESE trending half-graben during the Late Carboniferous–Early Permian. A significant angular unconformity occurs in the lower part of the Early Permian strata (Fig. 2; BRGM *1989*). Another discontinuity occurs around the boundary between Early and Late Permian (Fig. 2). Similar to other Late Paleozoic basins of the French Massif Central, the age of the continental sediments is poorly constrained (Feys *1989*; Broutin et al. *1986*) and the exact ages of these discontinuities are unknown. The possible Late Carboniferous sediments consist of gray to black sandstone and conglomerate. Paleobotanic studies indicate a Stephanian–Autunian or even possibly only Early Autunian age (Zeiller *1892*; Doubinger *1956*). Permian sediments, more than 500 m thick, are dominated by sandstone-clay alternations. The Early Permian is composed of the 30–40 m thick Saint-Antoine limestone, the gray–green–yellow-colored coarse Walchia sandstone and irregular alternations of red sandstone and red clay (Brive sandstone). The Saint-Antoine limestone is dated by *Estheria tenella* to be of Autunian age, and the Walchia sandstone by *Callipertis conferta* and *Lebachia piniformis* (Feys 1976). The Late Permian age of the other overlying continental formations is poorly controlled by facies correlation with the other Permian basins. These Late Permian (Saxonian-Thuringian) rocks are dominated by red continental sandstones with beds of regular thickness and variable hardness. The transition from Permian to Triassic is marked by coarse light colored sandstone and conglomerate (Fig. 2).

We collected 32 sites of Early Permian rocks for this study (Table 1). This collection can be lithologically separated into two parts: limestone of the lower part of the section (17 sites) and sandstone of the upper part (15 sites). Six to 15 oriented hand samples or mini drill cores per site were collected. Limestone is mainly exposed in the central part of the basin; only two limestone sites were sampled in the eastern and western parts (Fig. 1b). Because of poor outcrop quality, few sites in sandstone facies were collected in the western and central parts of the basin. Most of the sandstone collection consists of redbeds and only two sites are of gray–green–yellow color. Sites 49 and 50 are located in the southeastern extremity of the basin and near the contact with overlying Mesozoic cover (Fig. 1b). The solar and magnetic orientations, measured for core samples, are similar. Standard cylindrical cores were cut from hand samples in the laboratory (2.5 cm in diameter and 2.2 cm in length).

Site	Coordinates		Bedding strike/dip	Type of rocks	*n*/*N*	Before and after bedding corrections						Paleomagnetic pole			
	Latitude	Longitude				Dg	Ig	Ds	Is	k	α_{95}	λ	φ	K	A_{95}
A1	45.48°N,	1.28°E	horizontal	Limestone	8/8	192.9	−6.7	192.9	−6.7	601	2.0	46.6	162.5	1473	1.3
A2	45.48°N,	1.28°E	Horizontal	Limestone	10/10	193.7	−5.1	193.7	−5.1	319	2.5	45.6	161.5	606	1.8
A3	45.48°N,	1.28°E	Horizontal	Limestone	4/4	202.7	−6.6	202.7	−6.6	187	5.1	43.6	149.1	270	4.3
B	45.26°N,	1.38°E	255/11NW	Limestone	13/19	199.5	−5.2	199.4	3.9	34	6.6	39.7	155.9	57	5.2
C	45.29°N,	1.35°E	Horizontal	Limestone	8/9	187.3	−8.1	187.3	−8.1	63	6.2	48.3	170.3	88	5.3
F	45.25°N,	1.39°E	30/13E	Limestone	8/11	194.1	−9.1	196.5	−12.4	82	5.5	48.6	156.2	206	3.5
G	45.25°N,	1.38°E	230/8NW	Limestone	6/19	195.3	2.6	195.9	7.2	218	3.9	39.1	160.7	457	2.7
H	45.23°N,	1.41°E	Horizontal	Limestone	6/6	194.1	−2.7	194.1	−2.7	47	8.3	44.5	161.5	151	4.7
J	45.24°N,	1.41°E	Horizontal	Limestone	3/5	197.4	−7.1	197.4	−7.1	44	3.9	45.6	156.1	864	2.7
K	45.20°N,	1.41°E	Horizontal	Limestone	10/14	205.6	0.5	205.6	0.5	141	3.7	39.2	147.8	312	2.5
L	45.27°N,	1.40°E	70/4S	Limestone	12/13	186.5	−2.1	186.7	−5.7	103	4.0	47.2	161.6	187	3.0
M	45.22°N,	1.44°E	Horizontal	Limestone	6/8	199.5	4.8	199.5	4.8	21	12.4	39.2	155.8	36	9.6
N	45°22N,	1.44°E	Horizontal	Limestone	7/11	198.2	1.0	198.2	1.0	28	10.0	41.5	156.8	55	7.2
O	45.20°N,	1.43°E	180/5W	Limestone	8/12	195.6	1.6	195.7	0.2	28	9.4	42.6	159.9	45	7.3
P	45.19°N,	1.42°E	180/5W	Limestone	10/10	196.5	−1.4	196.3	−2.8	49	6.3	43.9	158.4	74	5.2
01[a]	45.13°N,	1.45°E	45–70/10–30	Redbeds	8/8	187.6	0.0	188.7	−12.7	46	8.2	50.6	167.8		
11[a]	45.17°N,	1.55°E	186/10NE	Redbeds	6/6	192.7	−2.0	192.3	−3.0	141	5.7	45.0	164.0		
12[a]	45.24°N,	1.35°E	111/3SW	Redbeds	6/6	193.5	−12.7	193.4	−15.7	153	5.4	51.0	160.2		
A: Western Basin					18	195.2	−3.2	195.4	−4.0	104	3.2	44.7	159.0	217	2.2
D	45.16°N,	1.64°E	215/45W	Limestone	7/17	188.3	−22.2	180.2	1.6	44	7.0	44.0	180.5	83	5.8
E	45.15°N,	1.64°E	110/3S	Redbeds	10/14	180.7	4.2	180.8	1.4	54	6.0	44.2	180.2	113	4.2
37	45.15°N,	1.65°E	80/35S	Redbeds	8/8	177.9	35.0	176.5	0.3	386	2.8	44.6	186.6	471	2.6
38	45.15°N,	1.67°E	96/33S	Redbeds	7/7	182.9	28.0	183.3	−5.0	161	4.8	47.3	176.8	353	3.2
39	45.14°N,	1.67°E	153/40S	Redbeds	6/6	174.4	9.7	175.7	−5.9	35	11.5	47.6	188.1	45	10.2
40	45.14°N,	1.68°E	126/20S	Redbeds	6/6	163.2	20.1	167.0	7.4	101	6.7	39.8	198.7	113	6.5
41	45.15°N,	1.62°E	81.4/36.4S	Redbeds	6/6	179.3	29.5	178.3	−6.6	108	6.5	48.1	184.2	171	5.1
42	45.15°N,	1.61°E	86.5/35S	Redbeds	8/8	178.0	36.1	177.7	1.1	117	5.1	44.3	184.8	135	4.8
43	45.15°N,	1.60°E	111.1/34.8S	Redbeds	6/6	185.7	24.1	186.9	−9.6	143	5.6	49.2	171.0	179	5.0
44A	45.15°N,	1.59°E	115.2/19.8S	Redbeds	6/6	182.6	3.7	181.8	−14.6	259	4.2	52.2	178.7	439	3.2
44B	45.15°N,	1.58°E	115/32S	Redbeds	6/6	181.5	38.6	186.6	8.6	41	10.6	40.2	173.0	80	7.5

Site	Coordinates		Bedding strike/dip	Type of rocks	*n*/*N*	Before and after bedding corrections						Paleomagnetic pole			
	Latitude	Longitude				Dg	Ig	Ds	Is	k	α_{95}	λ	φ	K	A_{95}
45	45.08°N,	1.65°E	115/25	Yellow-green sandstone	0/6	–	–	–	–	–	–	–	–	–	–
46	45.02°N,	1.75°E	115.8/23.3S	Redbeds	6/6	167.8	2.2	166.0	−16.0	66	8.3	51.2	204.2	95	6.9
47	45.02°N,	1.76°E	120/25S	Limestone	5/6	166.7	36.4	174.8	16.9	30	14.2	36.1	188.1	80	8.6
48	45.02°N,	1.77°E	143.9/39.6S	Grey sandstone	5/7	173.5	16.5	177.1	−4.9	81	8.6	47.4	186.0	83	7.4
B: Eastern Basin (except eastern border)					14	177.3	19.0	178.1	−1.8	56	5.0	45.8	184.4	111	3.6
49	45.04°N,	1.76°E	143.6/9.3	Redbeds	6/6	207.3	5.5	207.4	−2.8	29	12.6	40.1	144.8	48	9.8
50	45°05°N,	1.75°E	148.7/8.3	Redbeds	6/6	206.7	−4.5	206.1	−11.6	80	7.5	44.7	143.8	130	6.7
C: Eastern border					2	207.0	0.5	206.8	−7.2	–	–	42.4	144.3	–	–

Table 1 Early Permian (Autunian) paleomagnetic sampling and results from Brive basin

Abbreviations are n/N = number of entries in the statistics and number of demagnetized samples; D, I, k, α_{95},K, A_{95} are declination, inclination and Fisher (*1953*) statistic parameters; Subscripts g and s stand for geographical and stratigraphical coordinates; λ and φ are latitude and longitude of paleomagnetic pole. Strike is counterclockwise from downward dip. Angles are in degrees; [a] stands for the sites previously published (Chen et al. *1997*)

Anisotropy of magnetic susceptibility

Anisotropy of magnetic susceptibility (AMS) was measured with a KLY3 Kappabridge (AGICO, Brno, Czech Republic). The study of AMS has been carried out to make a knowledge on depositing horizontal and to detect possible posterior deformation (Blès et al. *1989*). Magnetic foliation poles (minimum susceptibility axes K_3) generally show steep inclinations (Fig. 3a) and are close to the poles of bedding planes. The magnetic lineations (maximum susceptibility axis K_1), are sub-horizontal and trend predominantly NW–SE. Most samples exhibit positive values of the shape parameter *T* (Jelinek *1981*), indicating a dominant planar fabric, but prolate fabrics were also observed in some samples (Fig. 3b). The

anisotropy degree P′ (Jelinek *1981*) is less than 1.05 for the majority of the samples (Fig. 3b). The orientation of the minimum axis is typical for sedimentary rocks (Hrouda 1982), but the presence of prolate fabrics and the NW–SE clustering of the maximum K_1 axes could be related to very weak deformations or depositional processes in this NW–SE trending basin. No strain or only very weak deformation affected these rocks, and a primary remanent magnetization could therefore have presented in these rocks.

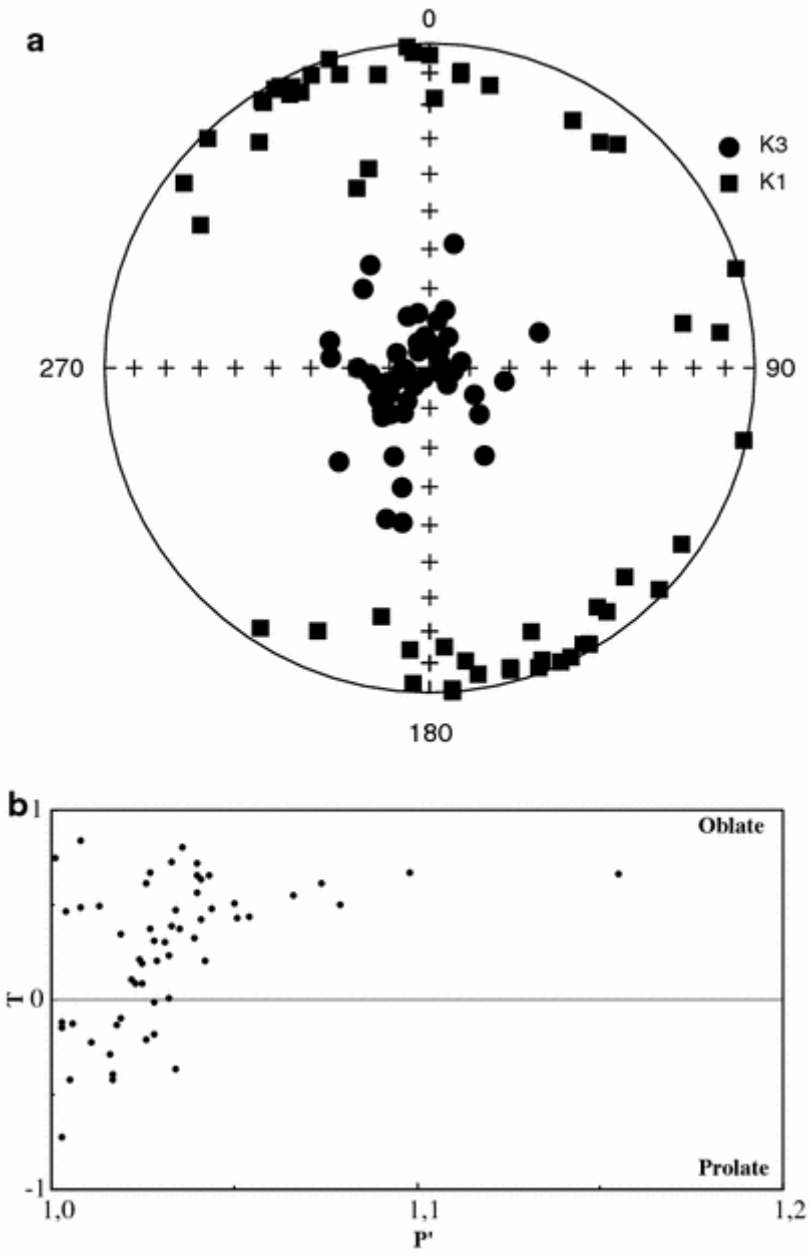

Fig. 3 AMS results. **a** Equal-area projection of maximal (K_1) and minimum (K_3) axes of AMS, **b** shape parameter (T) versus anisotropy degree (P') plot

Anisotropy of magnetic susceptibility measured on limestone samples yielded inconclusive results due to extremely weak bulk susceptibility to unacceptably large errors.

Magnetic mineralogy methods

To characterize the magnetic mineralogy, we conducted the following laboratory analyses: thermomagnetic behavior of low field susceptibility with the CS3 attachment of the KLY3 Kappabridge, magnetic hysteresis acquisition with a translation inductometer within an electromagnet, measurement of magnetic remanence with a JR5 or JR4 magnetometer (AGICO, Brno, Czech Republic) and demagnetization with a laboratory built furnace or LDA-3 alternative magnetic field demagnetizer (AGICO, Brno, Czech Republic). These analyses were carried out both in the Laboratoire de Magnétisme des Roches d'Orléans and the Laboratoire de Paléomagnétisme of Institut de Physique du Globe de Paris (Saint Maur). The magnetic remanent directions were isolated by principal component analysis (Kirschvink *1980*) and the mean directions computed by Fisher spherical statistics (1953) using paleomagnetic software packages offered by Cogné (*2003*), R. Enkin and M. Le Goff.

Limestone Thermomagnetic experiments reveal the presence of two principal magnetic minerals, magnetite and hematite, by significant drops of magnetic susceptibility at intervals of 530–580°C and 600–680°C, respectively (Fig. 4a). The hysteresis loops show a strong paramagnetic and/or high coercive magnetic mineral dominance with a linear trend at magnetic fields above 700 mT (Fig. 4b). After removing the paramagnetic effect, the magnetic hysteresis curve confirms the existence of a low coercive mineral like magnetite (Fig. 4c). Saturation is reached at about 170 mT (Fig. 4c). The ratios of Js/Jrs and Hc/Hrc are about 0.5 and 3.1, respectively. These values are typical for pseudo single domain titanomagnetite (Dunlop 1986).

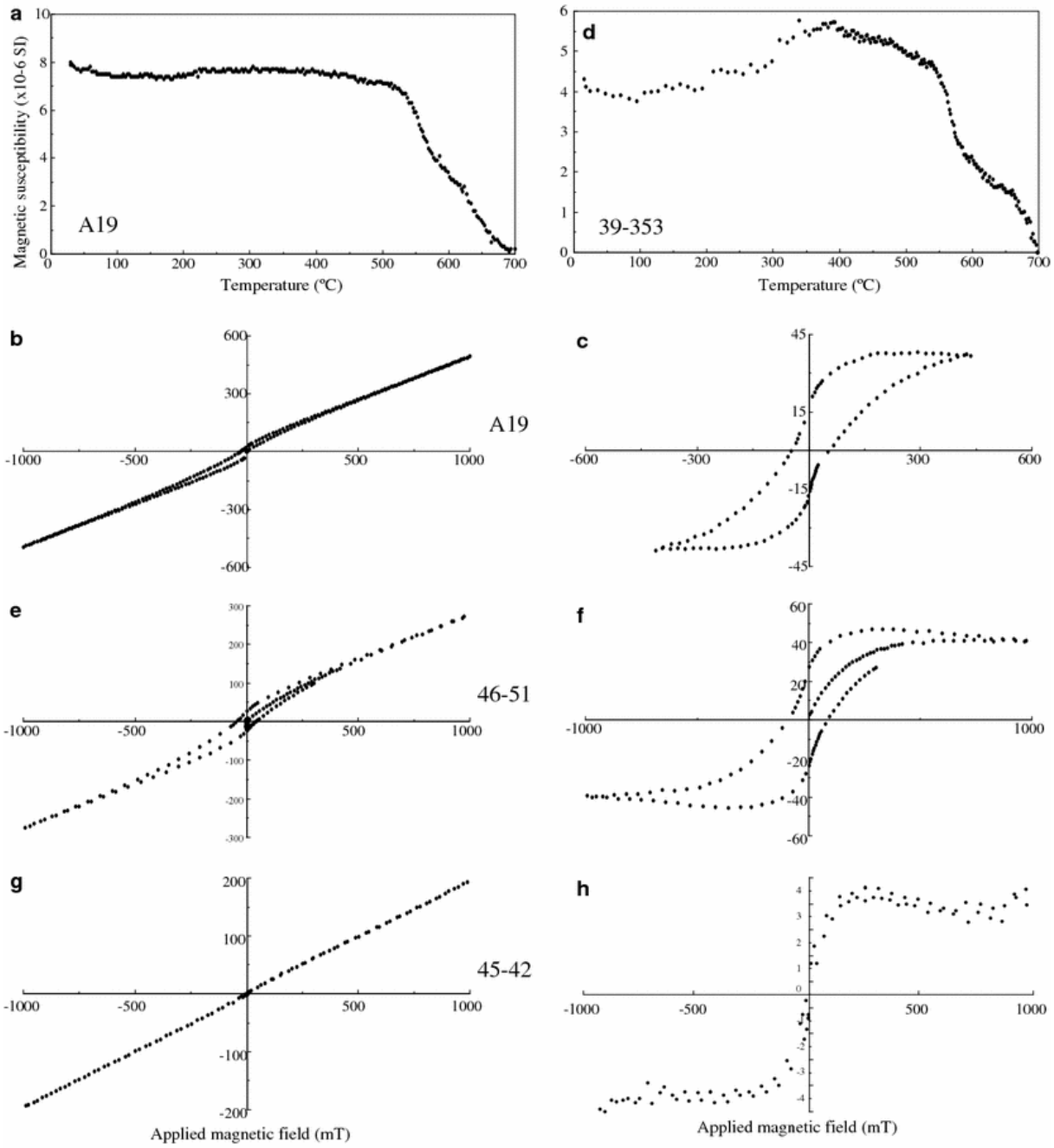

Fig. 4 Magnetic mineralogical studies on the representative samples by thermomagnetic and induced magnetic moment experiments

Sandstone More complicated magnetic behavior was observed in sandstone samples. Samples from the redbeds exhibit similar behavior as the limestones, though the thermomagnetic measurements show a weaker magnetic susceptibility than the limestones, and two susceptibility drops around 550–580°C and 650–680°C (Fig. 4d). The linearity at high magnetic fields of the hysteresis curves indicates the dominance of paramagnetic or high

coercive minerals (Fig. 4e). After the removal of paramagnetic slope, typical magnetite characteristics are revealed (Fig. 4f) with ratios Js/Jrs and Hc/Hrc about 0.6 and 2.5. These observations show that the main magnetic minerals are magnetite and hematite. The gray–green–yellow sandstones exhibit very weak susceptibility, close to the sensitivity of the susceptibility bridge. The hysteresis curve reveals an almost perfect linearity between the applied magnetic field and the induced magnetic moment (Fig. 4g). After subtraction of the paramagnetic slope, a small contribution of ferromagnetic minerals is observable (Fig. 4h). No reliable magnetic parameters, such as saturation moment or coercive force, can be determined, so the magnetic remanence carrier of this facies is indeterminable at this step.

Remanent magnetization analysis

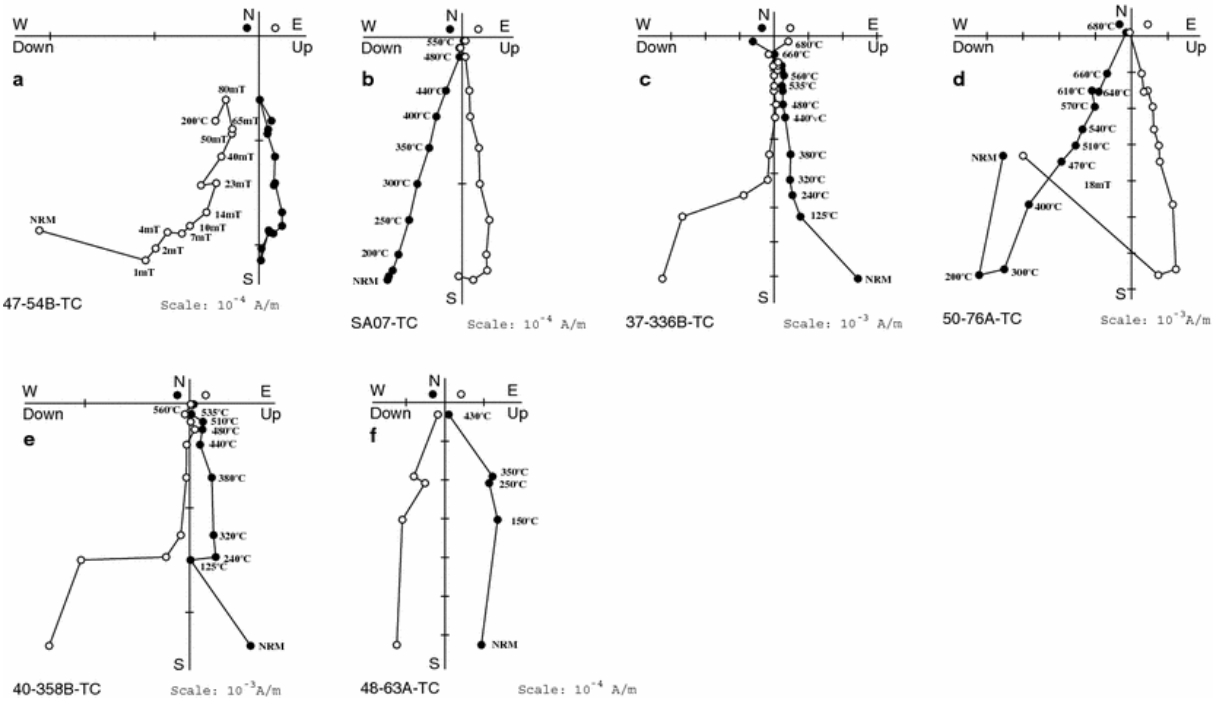

Fig. 5 Orthogonal projections of progressive demagnetization of representative samples (Zijderveld *1967*). *Solid* (*open*) symbols represent projection in horizontal (vertical) plan

The natural remanent magnetization (NRM) intensities of the limestone samples are weak, in the order of 10^{-4} A/m at the border of the basin, but often much lower in the dark facies of the central part of the basin. Alternating magnetic field (AF) demagnetization technique was tested on a few samples. Progressive demagnetization steps, varying from 1–15 mT, were

applied up to 80 mT (Fig. 5a). A poorly defined component is often removed from 0–10 mT and a relatively stable component is isolated from 10–80 mT (Fig. 5a). Most of the samples were then thermally demagnetized, allowing the determination of a stable component in the temperature range from 200–300°C to 450°C (Fig. 5b-5f). For part of the samples from the dark facies, the NRM was below the sensibility of magnetometer. All stable magnetic components are characterized by uniquely reversed polarity.

Sandstone specimens were treated by progressive thermal demagnetization with temperature intervals varying from 20 to 200°C. Redbed samples display a viscous component from room temperature to 300°C and a stable component at higher temperatures (Fig. 5b–5e). A stable magnetic component has been isolated from the majority of the redbed specimens in a temperature range from about 300 to 680°C (Figs. 5c, d), indicating that both magnetite and hematite carry coherent magnetic directions. The magnetic remanence of the specimens that were completely demagnetized by about 550°C may be carried only by magnetite or partially by hematite of coarser grain size (Figs. 5b, e). The two sites with gray–green–yellow colored sandstone show either a highly viscous magnetization (Fig. 5f) or are too weakly magnetized (Site 45). Again, the stable high temperature component presents only reversed polarity.

Discussion

Samples from 32 sampling sites yield stable magnetic components (Table 1). Fisher statistics (1953) of all site-mean directions shows a better grouped mean direction after bedding correction (index s) with respect to before (index g): N=34, Dg=188.9°, Ig=6.0°, kg=18, α_{95}g=5.7°; Ds=189.0°, Is=−3.4°, ks=38 α_{95}s=3.9° (Fig. 6a, b). The ks/kg ratio of 2.15 exceeds the critical value of 1.78 for the simple and stringent McElhinny (*1964*) fold test at 99% confidence level (folding occurred before Triassic time; Fig. 7). This positive-fold test is also obtained at 99% confidence level with the method proposed by McFadden (*1990*; ξ_1IS= 7.86, ξ_1TC= 4,94,ξ_2IS= 21.32; ξ_2TC= 0.65 and the 6.68 and 9.59 for critical values of 95 and 99% confidence levels, respectively). Proportional incremental unfolding according to Watson and Enkin (*1993*) confirms this conclusion with a maximum k value at 98.6% unfolding (Fig. 7). The solely reversed polarity of sites widely spread in both geographic distribution and stratigraphic position is consistent with the remanence being blocked during the Permian Kiaman Long Reversal Superchron. The obtained directions have lower inclination than those

obtained for the upper part of the Permian series (Chen et al. *1997*). Therefore, the age of the remanent magnetization probably corresponds to the stratigraphical age of the rocks. However, the distribution of the paleomagnetic directions shows a significant scatter in declination (Fig. 7b). This suggests either that differential vertical-axis rotations have occurred between these sites or that the age interval of the studied rocks is so large that scattering reflects the effect of continental drift. The second hypothesis can be excluded because neighboring sites of different age (limestone and red beds) give similar paleomagnetic directions. Therefore, the Brive basin experienced differential rotations and these differential rotations do not correspond to the intra-Autunian discontinuity (Fig. 2).

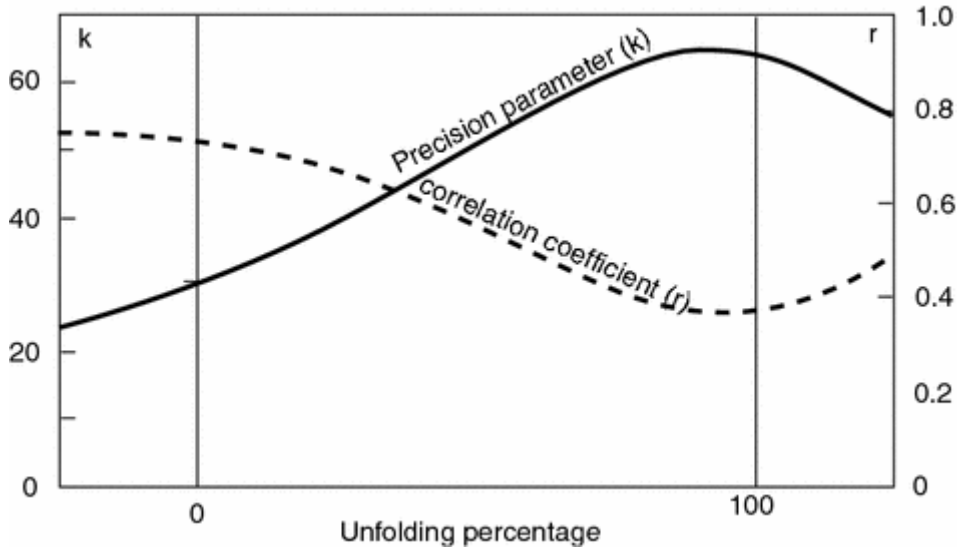

Fig. 6 Equal-area projection of site-mean paleomagnetic directions for zones A (*squares*), B (*circles*) and C (*triangles*) before **a** and after **b** bedding corrections. Open (*full*) *symbols* correspond to the upper (lower) hemisphere. The *bigger symbols* present the mean directions for corresponding groups. *Star* shows the present field direction at the sampling locality. A positive-fold test is concluded (see Table 1 and test)

When treating the Early Permian (Autunian) results, we divide the Brive basin into three parts from NW to SE (Table 1 and Fig. 1), each with coherent paleomagnetic directions: Areas A (n=18, Ds=195.4°, Is=−4.0°, ks=104 α_{95}s=3.2°), B (n=14, Ds=178.1°, Is=−1.8°, ks=56 α_{95}s=5,0°) and C (n=2, Ds=206.8°, Is=−7.2°). Areas A and B are separated by the Larche and Lissac strike-slip faults (Fig. 1b). Area C lies in the easternmost part of the basin, represented by only two sampling sites (Fig. 1b). The fold tests are indeterminate for area A (too weak variation of dip in this area) but significant at 99% for area B (ks/kg ratio of 2.9 exceeding the

critical value of 2.55 for the fold test of McElhinny (*1964*). Mean paleomagnetic poles were computed for each group (Table 1).

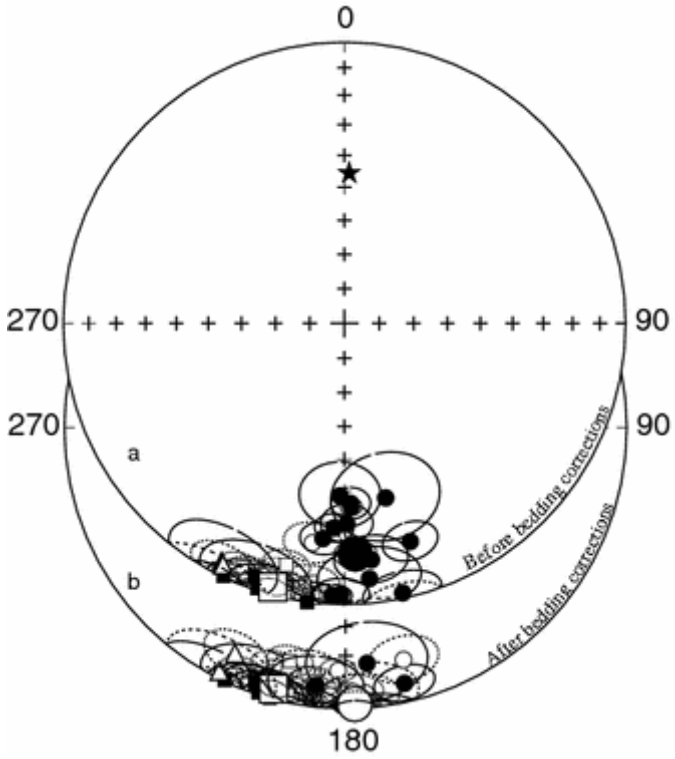

Fig. 7 Variations of the precision parameter (k, *solid line*) and of correlation coefficient (McFadden *1998*) (r, *dashed line*) for progressive unfolding from −25–125%. The highest k value is located at 98.6% of unfolding (Watson and Enkin *1993*)

Area A sites lie on both sides of the Segonzac strike-slip fault. Because all sites have similar paleomagnetic directions, this fault was therefore possibly not significantly active between the Autunian and the Late Permian. However, a significant counterclockwise rotation of 17.3° ±4.1° of area B with respect to area A was observed (De marest 1983; Fig. 8a). Because of the small number of sites from the area C, its rotation cannot be precisely defined with respect to area B. However, area C seems to have experienced a clockwise rotation of □30° with respect to area B. This relative rotation may have been produced by Mesozoic thrusting along the Meyssac fault. In other words, the rotation of area C is local, as this area is located on the extreme eastern corner of the basin. In contrast to the Autunian data, the declination scatter of the paleomagnetic directions is not observed in the Saxonian–Thuringian data (Fig. 8b) from 12 geographically well-distributed sites within the Brive basin (Chen et al. *1997*; Fig. 1b). The

apparent Fisher distribution of these poles implies that the Brive basin can be considered as a rigid block since that time (Fig. 8b). Therefore, the differential rotations observed for the Early Permian formation probably correspond to the discontinuity observed between the Early and Late Permian (Fig. 2). Thus, the Brive basin seems "welded" after the Autunian.

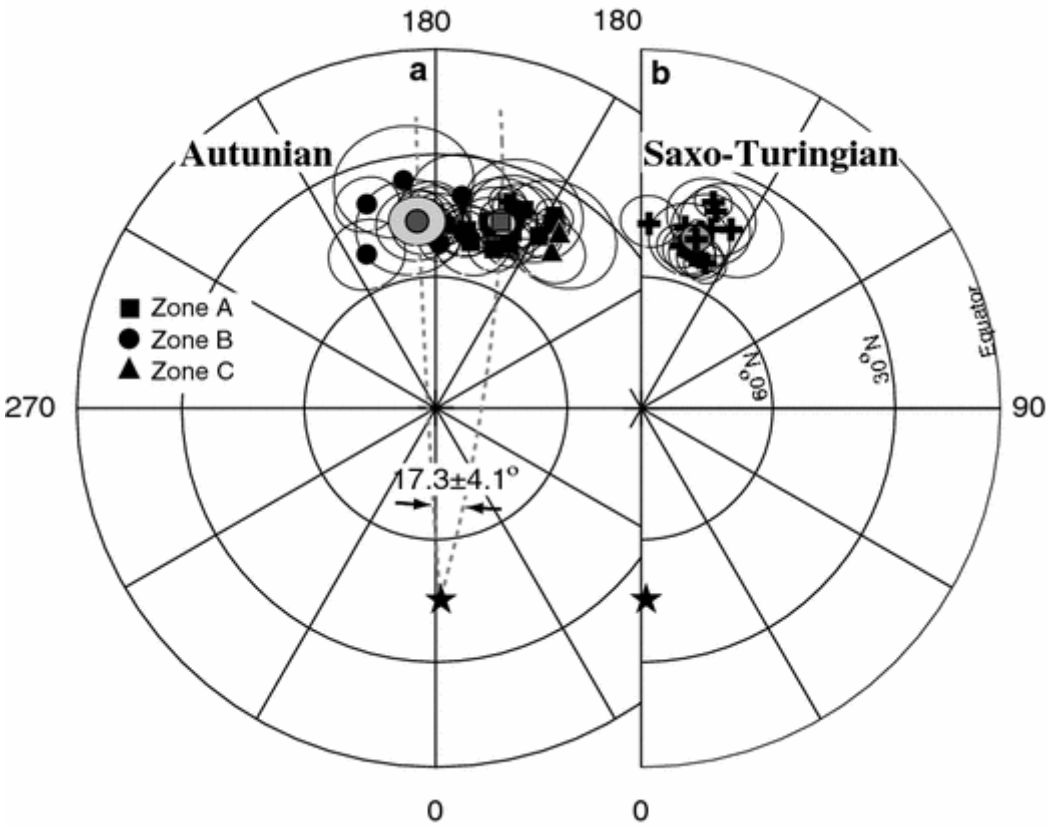

Fig. 8 Paleomagnetic poles of Early **a** and Late **b** Permian of the Brive basin. Distinguished poles are obtained from different zones of the Brive basin for the Autunian rocks, however, the Saxo-Turingian data show a better coherence

A summary of Permian paleomagnetic investigations from several continental basins of the French Massif Central: Brive, Largentière, Lodève, Rodez and Saint-Affrique was recently presented by Diego-Orozco et al. (*2002*; Table 2). Detailed statistical analyses of paleomagnetic data show that these five basins were positioned at similar equatorial latitudes. However, their declination pattern is more complicated. Relative rotations have been observed both at intra- and whole-basin scales. Figure 9 presents the rotations inferred for each studied basin of the French Massif Central with respect to Stable Europe (Diego-Orozco et al. *2002*).

The gray (black) arrows indicate the Early (Late) Permian paleomagnetic rotations, respectively. Two remarks can be made. The first one concerns the heterogeneity of rotations among these basins or within some basins in the Early Permian. The Brive and Saint-Affrique basins experienced significant internal deformation (Fig. 9, Table 2; Cogné et al. *1993*; Diego-Orozco and Henry *1993*; this study). However, the good consistency of paleomagnetic declinations of the Late Permian (Saxonian-Thuringian) rocks measured in the Rodez, Largentière and Lodève basins suggests that they behave as rigid bodies (Fig. 9, Table 2; Mérabet and Guillaume *1988*; Henry et al. *1999*; Diego-Orozco and Henry *1998*; Diego-Orozco et al. *2002*). This observation suggests that if major faults in the French Massif Central, such as the Sillon Houiller and Argentat faults, produced significant rotations in the Early Permian, this would not be the case after the Late Permian because of the paleomagnetically not detectable rotations between those basins which are separated by these major faults.

A close look at the distribution pattern of the Late Permian declinations shows that almost all declinations exhibit a slight counterclockwise rotation of each basin with respect to Stable Europe. Although these relative rotations are often statistically insignificant, their consistency suggests that the French Massif Central probably experienced a slight counterclockwise rotation with respect to Stable Europe after the Late Permian.

Site	Before tilt correction					After tilt correction							
	N	**D(°)**	**I(°)**	**k**	**α_{95}**	**D(°)**	**I(°)**	**k**	**α_{95}**	**lat. (°N)**	**long. (°E)**	**K**	**A_{95}**
LODEVE													
“Autunian"	5	192.6	17.9	442	3.0	190.6	8.1	411	3.1	41.3	169.3	464	2.9
“Saxonian"	3	190.4	15.3	351	4.3	190.1	3.5	351	4.3	43.7	169.5	666	3.1
“Thuringian"	6	198.9	−0.4	1361	1.5	199.4	−11.8	1361	1.5	48.6	153.5	2096	1.2
SAINT-AFFRIQUE													
2a (north)	3	173	(2.5	101	8)	172	(6	37	14)	–	–	–	–
2a (south)	6	196.6	(11.0	124	5.1)	195.9	(6.9	93	5.9)	–	–	–	–
2b	7	182.8	−3.9	545	2.3	182.5	0.4	393	2.7	45.9	179.2	978	1.7
Dourdou	8	184.4	13.1	30	9.1	183.6	−4.4	240	3.2	48.2	177.4	590	2.0
Saint-Pierre	8	192.3	−4.3	134	4.3	192.4	−8.4	114	4.6	48.9	163.8	325	2.7
LARGENTIERE													
II–IV	13	193.2	2.4	29	7.2	193.4	−2.7	55	5.2	45.4	164.9	89	4.1
RODEZ													
FIII	18	190.3	−6.0	22	7.0	190.0	−4.3	95	3.4	47.0	168.1	210	2.2
Grès Rouges	23	189.8	−12.0	22	6.1	190.2	−13.2	53	4.0	51.5	166.0	68	3.5
BRIVE													
Autunian A	18	195.2	−3.2	141	2.8	195.4	−4.0	104	3.2	44.7	159.0	217	2.2
Autunian B	14	177.3	19.0	19	8.6	178.1	−1.8	56	5.0	45.8	184.4	111	3.6
Autunian C	2	207.0	0.5	–	–	206.8	−7.2	–	–	42.4	144.3	–	–
“Saxo-Thur."	12	195.5	−18.8	32.1	7.8	192.6	−10.6	86.3	4.7	48.8	162.2	193.3	3.1

Number of sites (*N*), mean direction (D, I) before and after dip correction and paleomagnetic pole (lat., long.). Corresponding Fisher’s (*1953*) parameters (k, α95, K, A95). For data between parentheses, only the declination is reliable (Diego Orozco and Henry 1993).

Table 2 Paleomagnetic data from Permian basins of French Massif Central for each formation

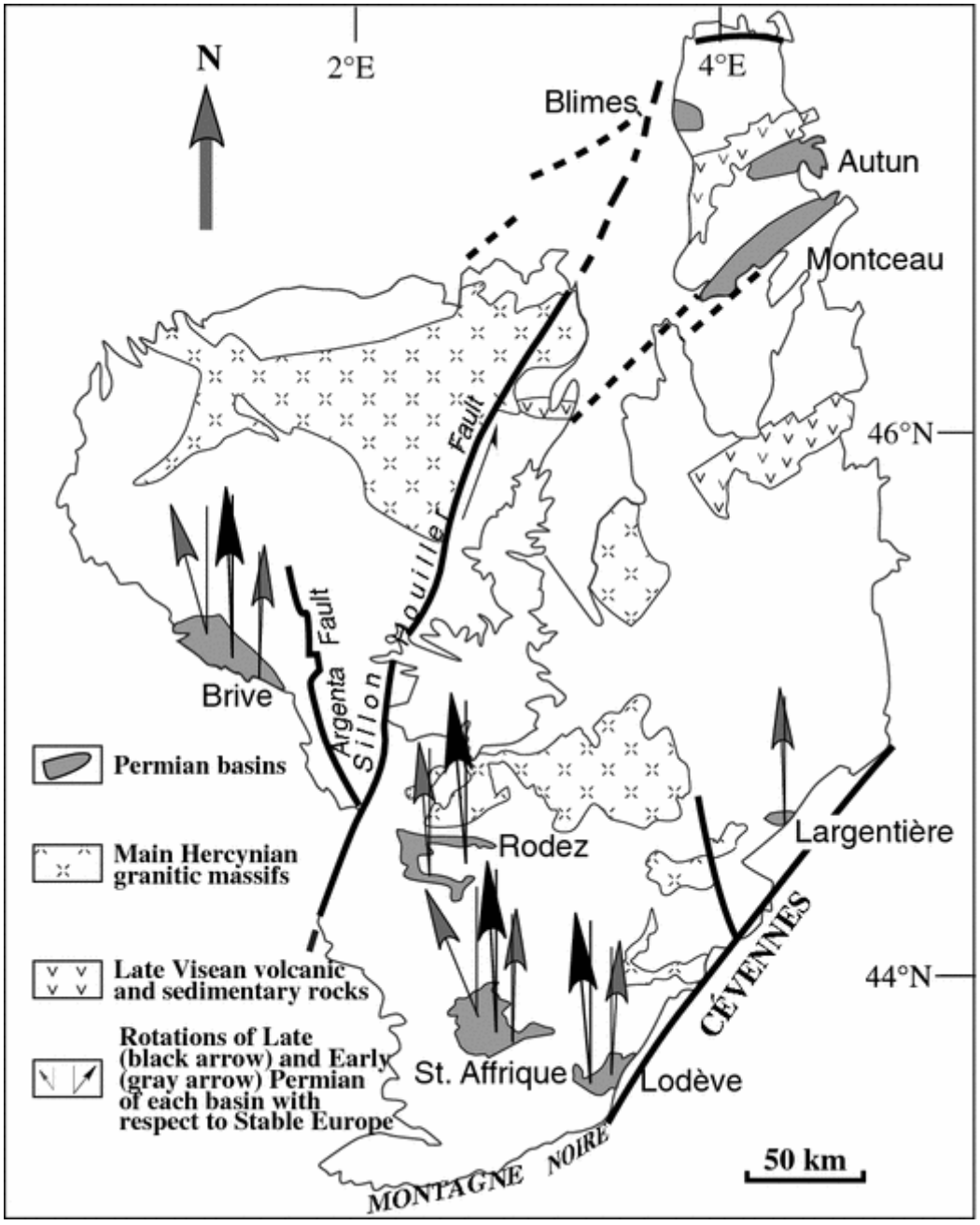

Fig. 9 A sketch of tectonic map of the French Massif Central with Early (*gray*) and Late (*black*) rotations of each basin with respect to Stable Europe (Van der Voo *1990*)

It also remains possible that "Stable" Northern Europe underwent very weak deformation during the Alpine (i.e., Meso-Cenozoic) orogeny and rotated clockwise. Another possibility is that the slight rotation of the French Massif Central might be related to movement along reactivated Variscan faults. Reactivation of the Sillon Houiller, Argentat or Villefort faults appears unlikely since they are located within the massif itself. Conversely, the Cévennes

fault which polyphased activity, in particular its sinistral wrench displacement during the Eocene Pyrenean compression, is well documented (e.g., Arthaud and Laurent *1995* and enclosed references) is a good candidate to accommodate the post-Permian rigid rotation of the French Massif Central with respect to stable Europe.

Conclusion

Thirty-two out of thirty-four sampling sites of Early Permian sandstone and limestone from the Brive basin show positive-fold tests and solely reversed polarities. We interpret the characteristic remanent magnetization as primary. The tilt-corrected site-mean declinations vary from 207° to 167° indicating that the Brive basin experienced internal vertical-axis rotations. On the contrary, Late Permian paleomagnetic site means exhibit a circular Fisherian distribution showing no relative rotations. Detailed analyses of Permian paleomagnetic data from five contemporaneous basins of the French Massif Central reveal that these basins share the same equatorial paleolatitude with stable Europe throughout the Permian. However, in Early Permian, three of the five basins experienced differential vertical-axis rotations. The Saint-Affrique basin not only suffered internal deformation during the Early Permian like the Brive basin, but also the basin as a whole underwent a counterclockwise vertical-axis block rotation with respect to stable Europe. The data from Late Permian rocks show well-consistent paleomagnetic directions, thus no evidence for significant deformation between these basins. This emphasizes the importance of widely spread sampling in late orogenic basins in order to detect such events. On the other hand, paleomagnetic data obtained in newly accreted terranes (e.g., McElhinny et al. *2003*) have to be considered particularly with care to establish APWP.

Acknowledgements

This work was supported by the GéoFrance 3D program program and by Geodynamics of the internal Earth of International Innovative Team Project of Chinese Academy of Scicens. We are very grateful to H. Waldhör, J.-P. Cogné, J.-Cl. Soula and an anonymous reviewer for constructive and helpful comments. We present our thanks to Dr. S. Gilder for improving the manuscript.

References

Arthaud F, Laurent PH (1995) Contraintes, déformation et déplacement dans l'avant-pays Nord Pyrénéen du Languedoc méditerranéen. Geodinamica Acta 8:142–157

Autran A, Cogné J (1980) La zone interne de l'orogène varisque dans l'ouest de la France. Mém BRGM 108:90–111

Blès JL, Bonijoly D, Castaining C, Fros Y (1989) Successive post-Variscan stress fields in French Massif Central and its borders (Western European plate): comparison with geodynamic data. Tectonophysics 169:79–111

Bourges P (1987) Sédimentation alluviale et tectonique extensive dans le Permien du détroit de Rodez, Thesis, Toulouse, p 186

BRGM (1989) Synthèse géologique des bassins permiens français Ed BRGM 128:288

Broutin J, Doubinger J, Langiaux J, Primel D (1986) Conséquences de la coexistence de flores à caractères stéphaniens et autuniens dans les bassins limniques d'Europe occidentale. Mem Soc Géol France 149:15–25

Chen Y, Faure M, Cogné J-P (1997) Late Permian paleomagnetic results from the Brive basin (massif Central, France). Tectonophysics 281:209–220

Cogné J-P (2003) A Macintosh™ application for treating paleomagnetic data and making plate reconstructions. Geochem Geophys Geosyst 4:1007 DOI:10.1029/2001GC000227

Cogné J-P, Brun JP, Van Den Driessche J (1990) Paleomagnetic evidence for rotation during Stephano-Permian extension in southern Massif Central (France). Earth Planet Sci Lett 101:272–280

Cogné J-P, Van Den Driessche J, Brun J-P (1993) Syn-extension rotations in the Permian SaintAffrique basin (Massif Central, France): paleomagnetic constraints. Earth Planet Sci Lett 115:29–42

Demarest HH (1983) Error analysis for the determination of tectonic rotation from paleomagnetic data. J Geophys Res 88:4321–4328

Dewey J, Burke KC (1988) Tibetan, Variscan and Precambrian basement reactivation: products of continental collision. J Geol 81:683–692

Diego-Orozco A, Henry B (1993) Paleomagnetic results from the Permian Saint-Affrique basin (France) and implication for late and post-Hercynian tectonics. Tectonophysics 227:31–47

Diego-Orozco A, Henry B (1998) Données paléomagnétiques du bassin permien de Rodez et rotations dans la bordure sud-ouest du Massif central. C R Acad Sci Paris 327:225–229

Diego-Orozco A, Chen Y, Henry B, Becq-Giraudon F (2002) Paleomagnetic results from Permian Rodez basin implications: the late Variscan tectonics in the southern French Massif Central. Geodynamica Acta 15:249–260

Doubinger J (1956) Contribution à l'étude des flores autuno-stèphaniennes. Mém Soc Géol France 5:75

Dunlop D Özdemir Ö (1997) Rock magnetism. Cambridge University press, p 576

Faure M (1995) Late orogenic Carboniferous extensions in the Variscan French Massif Central. Tectonics14:132–153

Feys R (1978) Le Permien et la phase saalienne dans le bassin de Brive (SW de la France). In: Falke H (eds) "The continental Permian in the Central, West and South Europe". Reidel Publishing Company, Dordrecht, Holland, pp 80–90

Feys R (1989) Le bassin de Brive: in Synthèse géologique des bassins permiens français. Mém BRGM 128:78–84

Feys R, Guillot PL, Lefavrais A (1979) Tectonique du bassin de Brive. Bull BRGM 1:121–130

Fisher R (1953) Dispersion on a sphere. Proc R Soc Lond 217:295–305

Grolier J, Letourneur J (1968) L'évolution tectonique du Grand Sillon Houiller du Massif Central français. Proc 23rd Int Geol Cong I:107–116

Henry B (1988) Possibilitès et limites de la méthode paléomagnétique pour les corrélations stratigraphiques. 3éme Journées thém Assoc Géol Permien, Paris

Henry B, Becq-Giraudon F, Rouvier H (1999) Paleomagnetic studies in the Permian basin of Largentière and implications for the Late Variscan rotations in the French Massif Central. Geophys J Int 138:188–198

Henry B, Rouvier H, Le Goff M (2004) Using syntectonic remagnetizations for fold geometry and vertical axis rotation: example of the Cévennes border (France). Geophys J Int 157:1061–1070

Jelinek V (1981) Characterization of the magnetic fabric of rocks. Tectonophysics 79:63–67

Kirschvink JL (1980) The least squares line and the analysis of paleomagnetic data. Geophys J R Astron Soc 62:699–718

Lefavrais-Raymond A, Freys R (1976) Carte géologique de la France à 1/50 000 Brive-la-Gaillard. BRGM edition

Matte P (1986). La chaîne varisque parmi les chaînes paléozoïques péri-atlantiques modèle d'évolution et position des grands blocks continentaux au Permo-Carbonifère. Bull Soc Gèol Fr 8:9–24

McElhinny MW (1964) Statistical significance of the fold test in paleomagnetism. Geophys J R astron Soc 8:338–340

McElhinny MW, Powell CMcA, Pisarevsky SA (2003) Paleozoic terranes of eastern Australia and the drift history of Gondwana. Tectonophysics 362:41–65

McFadden PL (1990)A new fold test for palemagnetic studies. Geophys J Int 103:163–169

McFadden PL (1998)The fold test as an analytical tool. Geophys J Int 135:329–338

Mérabet N, Guillaume A (1988) Palaeomagnetism of the Permian rocks of Lodève (Hérault, France). Tectonophysics 145:21–29

Van der Voo R (1990) Phanerozoic paleomagnetic poles from Europe and North America and comparisons with continental reconstructions. Rev Geophys 28:167–206

Watson G, Enkin R (1993) The fold test in paleomagnetism as a parameter estimation problem. Geophys Res Lett 20:2135–2137

Zeiller R (1892) Bassin houiller et permien de Brive. Et. Gîtes minéraux France II. Flore fossile

Zijderveld JDA (1967) Demagnetization of rocks: analysis of results. In: Collision DW, Créer KM, Runcorn SK (eds) Methods in Paleomagnetism, pp 254–286